An organic-inorganic hybrid coagulant containing Al, Zn and Fe (HOAZF): preparation, efficiency and mechanism of removing organic phosphorus

Y. Fu and Y. Z. Wang

ABSTRACT

A polymeric-Al-Zn-Fe (PAZF) coagulant showing high removal of pollutants has been successfully developed using a galvanized slag in earlier works, but it gave less elimination of phosphorus. To improve phosphorus removal, a hybrid organic-Al-Zn-Fe (HOAZF) coagulant was prepared using PAZF and polyacrylamide (PAM) as an organic additive, and then was characterized by scanning electron microscopy (SEM), infrared spectroscopy (IR), X-ray diffraction (XRD), and Zeta potential, respectively. Removing efficiency and mechanism of organophosphorus by HOAZF was probed using jar tests in treating a simulated pesticide wastewater containing dichlorvos (DDVP), compared to that by PAZF and polyaluminum chloride. The results displayed that HOAZF having relative lower Zeta potential (compared to PAZF) exhibited complex surface morphology composited by Al, Zn and Fe and PAM, forming some new crystalline and amorphous substances different from that in PAZF. HOAZF gave higher removal of organophosphorus and far lower dosage than PAZF, and also posed a suitable wider pH range (pH = 7–12 for HOAZF and 10–11 for PAZF, respectively) and suitable wider organophosphorus level range than PAZF. Removing organophosphorus by HOAZF was a simultaneous complex process involving a non-phase transfer of adsorption/bridging/sweeping and a phase transfer of chemical precipitation.

Key words | coagulant, galvanized slag, HOAZF, organophosphorus, PAM, pesticide wastewater

Y. Fu (corresponding author)
Y. Z. Wang
School of Civil Engineering and Architecture,
University of Jinan,
Jinan 250022,
China
E-mail: *cea_fuy@ujn.edu.cn*

INTRODUCTION

More and more lakes and reservoirs suffer from serious eutrophication pollution worldwide with the increasing population, especially in China (Liu *et al.* 2014; Strokal *et al.* 2014). It has been widely recognized that eutrophication phenomenon emerges as total phosphorus reaches 0.015 mg/L (Ye *et al.* 2009), moreover, aquatic ecosystems show a high sensitivity to phosphorus limitation characteristics (limiting ratio of nitrogen and phosphorus) (Zhang *et al.* 2004). In addition, phosphorus is one of the key factors to avoid an outbreak of eutrophication extension (Schindler *et al.* 2008; Schelske 2009) because phosphorus can be easily removed from wastewaters (Schindler *et al.* 2008; Li & Brett 2015) by chemical, physicochemical or biological technologies due it not turning into a gas (N is often removed from wastewaters by becoming gas), so phosphorus removal (PR) has been extensively investigated (Li & Brett 2015).

The existing form of phosphorus in wastewater is mainly dependent on the types of wastewater, in which the most common form includes phosphates, polyphosphates and

doi: 10.2166/wrd.2017.115

organophosphorus. Generally, orthophosphate and polyphosphate are often soluble in water. Organophosphorus mostly exists in water in the form of colloid, particulates or dissolved organic phosphorus (Li *et al.* 2002; Mudryk *et al.* 2015). One of the main sources of organophosphorus in water is the use of organophosphorus pesticides (Ding *et al.* 2013; Zielinski & Jekatierynczuk-Rudczyk 2015) which is an important pesticide widely used around the world, resulting in frequent exceedance of the concentrations of organophosphorus pesticides over the maximum contamination level in water environments (Baldwin 2012; Li *et al.* 2016).

Presently, more than 80% of pesticides used in China are organophosphorus pesticides, resulting in severe damage to the entire water body. Currently, the technologies to remove total phosphorus (including organophosphorus, etc.) mainly involve physicochemical and biological methods. The former involves chemical precipitation, adsorption, coagulation precipitation (Huerta-Fontela *et al.* 2008; Saini & Kumar 2016), advanced oxidation (Badawy *et al.* 2006; Li *et al.* 2016), crystallization, electrolysis, membrane, etc. Chemical precipitation is mainly used to remove inorganic phosphorus, but has a larger amount of sludge (Meng *et al.* 2012). Adsorption is generally used to treat wastewaters with low phosphorus levels. Electrolysis often results in a lower removal of dissolved organophosphorus. Biological methods, which are generally used to treat wastewaters with low phosphorus concentration, do not show good stability and often give poor results (Qiu 2000). The requirement for phosphorus emission is strict now, for instance, the maximum phosphorus level in industrial effluents in China is 0.5 mg/L (Pan *et al.* 2004), and the discharging limit for total phosphorus in protected waters in some areas of Europe are 50 μL (EU 2000; Remy *et al.* 2014). So it is difficult to meet the emission requirement using one type of technology alone, thus leading to more and more hybrid processes (Du *et al.* 2015). As one of the pretreatment or advanced treatment methods, coagulation has been widely used due to its low cost (Zhou *et al.* 2015), and the investigations on efficient coagulants is still an important topic (Heiderscheidt *et al.* 2013; Zhou *et al.* 2015), especially in China.

Using various solid wastes to prepare inorganic and organic coagulant has been widely studied in the field of water and wastewater treatment (Fu *et al.* 2012; Zhou *et al.* 2015) due to serious solid waste pollution (Li *et al.* 2011). In a previous publication, polymeric-Al-Zn-Fe (PAZF) using galvanized-aluminum slag (generated from a surface chemical treatment of metals and other materials) was successfully developed and achieved some useful results (Fu *et al.* 2012, 2014). However, it was found PAZF did not have any advantages in PR compared with polyaluminum chloride (PAC) which has been extensively used for several decades around the world due to excellent coagulation behavior (Cao *et al.* 2012; Zhang *et al.* 2015). So to improve the efficiency of removing phosphorus by PAZF, the modification of PAZF was mainly investigated in this work.

In this work, a hybrid organic-Al-Zn-Fe (HOAZF) coagulant was prepared using polyacrylamide (PAM) (one of the organic flocculants and sludge conditioning agents widely used (Yan *et al.* 2013)) as a modifier (aiming at simplifying the dosing procedure of coagulants), and was characterized. The removal efficiency of organophosphorus by HOAZF was probed using jar tests in treating a simulated wastewater containing DDVP, in comparison with that by PAZF and PAC. The removing mechanism of organophosphorus by HOAZF was also analyzed. This work will provide some basic data for removing organic phosphorus with a new type of coagulant and will also put forward the possibility of using recycled galvanized-aluminum slag.

MATERIALS AND METHODS

Preparation of HOAZF

The galvanized aluminum slag from Zibo (China) was composed of the following components: $w(\mathrm{Al}) = 60\%$, $w(\mathrm{Zn}) = 38\%$, and $w(\mathrm{Fe}) = 2\%$.

The preparation of PAZF has been reported in previous publications (Fu *et al.* 2012, 2014).

HOAZF was prepared by a two-stage method of 'leaching with a mixed acid and polymerizing and compositing with alkali'.

Leaching stage with a mixed acid

HCl solution (8–15% (w/w), analytical grade) and H_2SO_4 solution (20–40% (w/w), analytical grade) were introduced rapidly into 3 g galvanized aluminum slag which was

smashed into smaller irregular-bulk material with an equivalent diameter of approximately 0.5–2 cm, and was followed by leaching for 1–3 h in a SHA-B Water Bath Constant Temperature Oscillator (Jintan Ronghua Instrument, China) at 80–90 °C to obtain a leaching solution. The leaching solution was then filtrated with ash-free quantitative filter papers (w(ash) < 0.01%, Whatman, UK) at 40–50 °C to obtain a color-free filtrate (Fu *et al.* 2012).

Polymerizing and compositing stage with alkali

PAM solution (0.1% (w/w) was introduced in the color-free filtrate in the previous section (PAM/color-free filtrate = 1/4 (v/v), analytical grade) under stirring for 5 min to obtain a mixing solution. NaOH solution (5% (w/w), analytical grade) was then added slowly into the mixing solution to composite for 5–72 h at 70 °C and stirred to obtain a light-brown liquid product of HOAZF with pH 2.5–3.0. The qualities of the liquid HOAZF were as follows: $w(Al_2O_3)$ of 4.59%, w(Zn) of 1.15%, w(Fe) of 0.26%, density of 1.1 kg/L, and basicity of 4.52%.

Liquid HOAZF was dried at 60–70 °C in an oven for more than 48 h and was made into powder samples for the following characterization. PAC ($w(Al_2O_3) = 29\%$) was purchased from Gongyi in Henan province in China. Double-deionized water was used to make all the following solutions.

Characterization of HOAZF

Surface morphology by scanning electron microscopy (SEM)

The surface morphology of solid HOAZF was observed and analyzed by SUPRA™ 55 FESEM (Zeiss, Germany) at 10 and 20 K magnification times under the following conditions: schottky field emission electron source, accelerating voltage 2–3 kV, in-lens SE detector, and electron beam booster.

Surface functional group analysis by infrared (IR) spectra

The surface functional group characteristics of solid HOAZF were analyzed by KBr pressed disc with Nicolet 380 IR Spectrum Meter (Thermo, USA).

Crystal characteristics by X-ray diffraction (XRD) spectra

The crystal characteristics of solid HOAZF were analyzed by D8 ADVANCE XRD (German BRUKER-AXS Ltd) with a voltage of 40 kV and scanning speed 2θ of 5 °/min, respectively.

Zeta potential

The Zeta potentials of liquid HOAZF and PAZF diluted 10 times were measured (Li 2012) five times by a 300HS potential and nano-particle size analyzer (Malvern, UK) at a temperature of 25 °C.

The pH of liquid HOAZF and PAZF diluted 10 times were adjusted to different values, and then their Zeta potentials were measured three times and the results represented the averages.

Organic PR by HOAZF

The simulated wastewater was made using an organophosphorus pesticide, O,O-dimethyl-O-(2,2-2 vinyl chloride) phosphate (DDVP, Shandong, China): 120 g DDVP was added to a mixed water of 15 L tap water and 5 L fountain water, and was followed by stirring for 30 min. The supernatant was then withdrawn after settling for 30 min as the tested wastewater with the following qualities: turbidity of 53.5 NTU, pH of 5.1–5.2, temperature of 22 °C, COD_{Cr} of 3,690 mg/L, and total phosphorus of 664.8–676.3 mg/L. Some fountain water was added to the tested wastewater in order to make it similar to the real wastewater samples.

The tested wastewater in this work mainly contained organophosphorus (DDVP) which was slightly water-soluble, so DDVP is not easily hydrolyzed after adding to the water. Although some inorganic phosphorus may be formed due to the addition of some fountain water when preparing the tested wastewater, the concentration of inorganic phosphorus was very low. Therefore, it is still considered that this tested wastewater mainly consisted of much more organophosphorus, and a small amount of dissolved inorganic phosphorus, turbidity substances and other organic matters. For the convenience of analysis, total phosphorus was measured instead of organophosphorus in the following experiments, and

organophosphorus (including a little inorganic phosphorus) removal was expressed in terms of PR.

A conventional jar test was performed using a six-unit stirrer system (ZR4-6 coagulation tester, Shenzhen Zhongrun, China). The standard jar test procedure consisted of a rapid mix at 200 rpm for 1 min after coagulant addition; followed by a 10 min mixing period at 50 rpm, and then the flocs were allowed to settle for 15 min. Then the supernatant were taken out for the analysis of turbidity and total phosphorus with a 2100AN Turbidity Meter (HACH, USA) and antimony molybdenum spectrophotometry. Three runs were conducted in the following tests, and the results represent the averages.

Influence of dosage

Dosage ranged between 0.685 and 6.85 mmol/L (as Al amount in the tested wastewater).

Influence of coagulation pH

The simulated wastewater was adjusted to 4–12 pH using NaOH or HCl solutions, respectively. Dosage was selected to be 4.11 mmol/L.

Influence of phosphorus level

The simulated wastewater was diluted to obtain the tested samples with different phosphorus levels varying between 41.1, 80.1, 163.8, 333.4 and 664.8 mg/L and pH values of 8.0, 7.6, 7.0, 6.1 and 5.1, respectively.

RESULTS AND DISCUSSION

Micro-characteristics of HOAZF

Surface morphlogy

Figure 1 displays the surface morphology of HOAZF at 10 K (Figure 1(a)) and 20 K (Figure 1(b)) magnification times, respectively. As shown in the previous studies (Fu *et al.* 2012), the surface morphology of PAZF presented a kind of uniform network structure consisting of some sort of cauliflower head of small size, with the characteristics of a large surface area having strong absorbability. However, as seen in Figure 1, HOAZF (showing different surface structure at different magnification times) exhibited significantly different surface morphology from PAZF. When the magnification time was 10 K (Figure 1(a)), HOAZF was mainly composed of some irregular stalactite-like or cotton-wad-like morphology, together with some irregular crevice-like or hole-like structures loosely distributed. The inner details of the hole-like structures were displayed at a magnification of 20 K (Figure 1(b)): the inner surface was composed of smooth flat-like, small size spherical-like, irregular protrusions structures, in which some holes were interconnected, and the edge of the holes were composed of irregular crystal-like, moss-like and different size of cotton-wad-like structures.

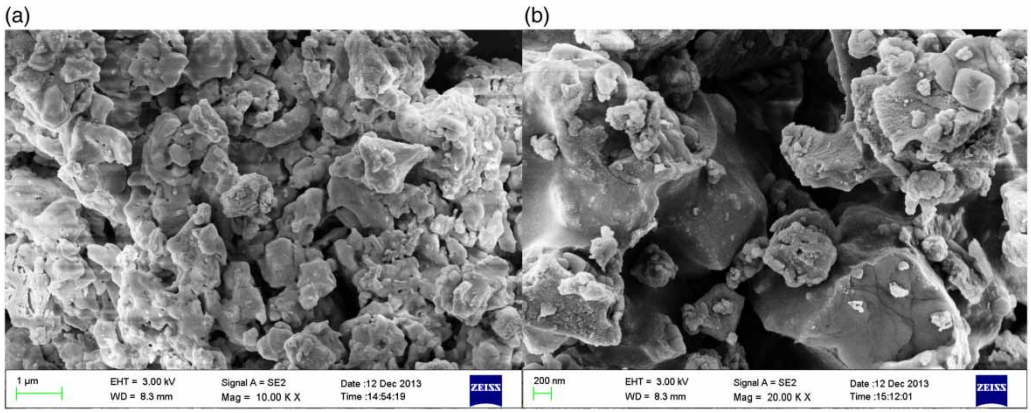

Figure 1 | SEM pictures of HOAZF. (a) ×10k, (b) ×20k.

The difference of the surface morphology of HOAZF from that of PAZF (Fu *et al.* 2012) may be originated from the chemical reaction between the various elements in the former. Complex composite reaction possibly occurred between PAM and Zn, Al, Fe, and some anions, etc., thus forming very complex complexes in HOAZF.

Surface functional group

Figure 2 displays the IR spectra of HOAZF.

The absorption at 3,416 cm^{-1} can be assigned to the stretching vibration of –OH (intermolecular hydrogen bonds) attached to Al in HOAZF (Lu & Deng 1989). The peak at 1,638 cm^{-1} can be attributed to the bending vibration of water absorbed, polymerized and crystallized in HOAZF (Lu & Deng 1989; Tan *et al.* 2011). The series of peaks at 844 and 1,258 cm^{-1} can be assigned to the bending vibration of Al-O-Al in the form of an octahedron, in which Al in the Al-O-Al bond may be replaced by Zn or Fe, forming more Zn-O-Al or less Fe-O-Al bonds, suggesting that Zn and Fe were polymerized with Al in HOAZF (Tan *et al.* 2011). The absorption from 555 to 659 cm^{-1} can be assigned to the vibration of Zn-O or Al-O in the octahedral of HOAZF. The peak at 1,112 cm^{-1} can be attributed to the stretching vibration of bridging-oxygen, probably being the vibration absorption of Al-O-Al, Zn-O-Zn, Zn-O-Al or Fe-O-Al, Zn-O-Fe bond (Kim *et al.* 2004). Within 400–800 cm^{-1}, the absorption of HOAZF gave a larger difference from that of PAZF (Fu *et al.* 2012) in which the former spilt out many small peaks; some changes probably occurred in the structure of HOAZF due to the composite reaction between organic and inorganic matters. In addition, the stretching vibration absorption peak of C = C double bond was not presented in 998 cm^{-1} (Zhao *et al.* 2010), suggesting that a rather complex composite reaction occurred between PAM and the inorganic metal ions, in which the monomer substance of acrylamide did not appear.

Crystal characteristics

XRD is an analytical method to study spatial distribution of atoms inside materials. As shown in Figure 3, crystalline characteristics were observed in HOAZF, in which some peaks showed the structure of NaCl (oval label in Figure 3) and others were unknown. No crystals of oxides or salts of Al, Zn, Fe, such as $Fe_2(SO_4)_3$, Fe_2O_3, $Fe(OH)_3$, Fe_3O_4 and so on, can be detected in HOAZF. The characteristic diffractive peak of PAM was also not detected at 20–23° of 2θ. This suggested that a complex composite reaction occurred between Al, Zn, Fe and PAM, forming one or many new crystalline substances, consistent with the results in Figure 2. Some 'wave-like peaks' appeared in some regions (such as, from 14 to 26° of 2θ, 32–44° of 2θ, and 47–64° of 2θ), instead of crystalline characteristics, indicating that some diffusive amorphous complexes of metals were formed in HOAZF, which was similar to that in PAZF (Fu *et al.* 2012).

Zeta potential

Table 1 displays the Zeta potentials of HOAZF and PAZF, and Figure 4 shows the Zeta potentials of HOAZF and PAZF at different pH values.

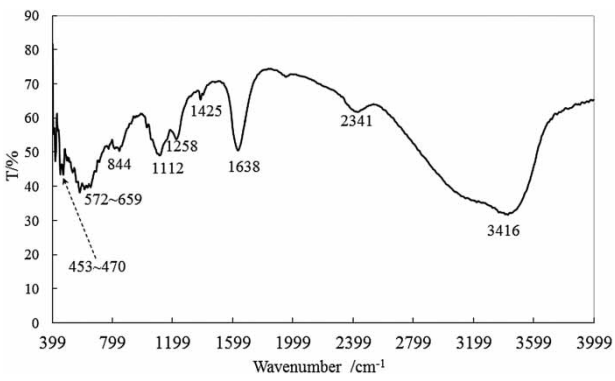

Figure 2 | IR spectra of HOAZF.

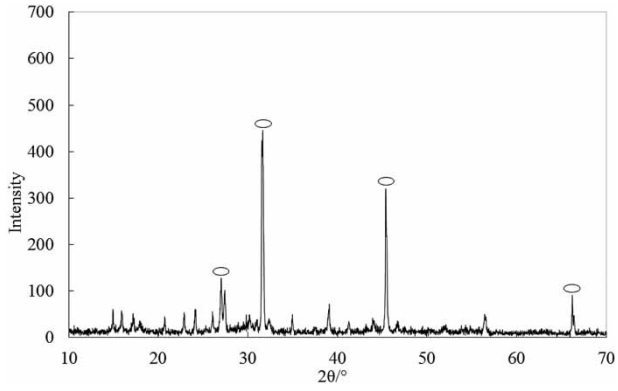

Figure 3 | XRD spectra of HOAZF.

Table 1 | Comparison of Zeta potential between HOAZF and PAZF (mV)

Coagulants	Zeta potential				Averages		Range
HOAZF	36.8	32.2	38.5	33.8	37.5	35.8	6.3
PAZF	41	44.4	43.2	42.6	43.8	42.9	3.4

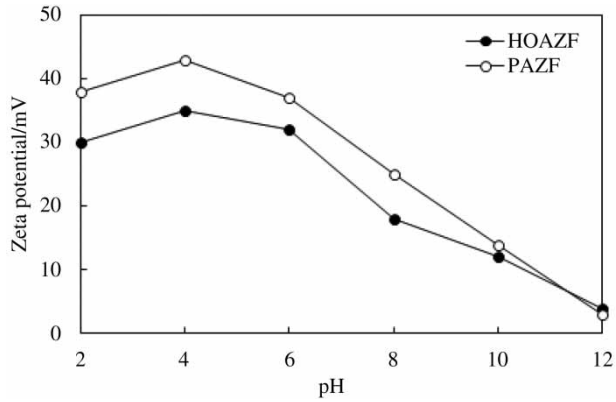

Figure 4 | Zeta potentials of HOAZF and PAZF at different pH values.

As seen from Table 1, the Zeta potentials of both HOAZF and PAZF were much larger than the isoelectric point (net charge equivalent to 0 mV), in which the Zeta potential of HOAZF was lower than PAZF and the degree of uniformity of charge distribution on various species of HOAZF was smaller than that of PAZF (as seen from the different changes in Zeta potential between different pH ranges) due to the additon of PAM.

As seen from Figure 4, the Zeta potentials of both HOAZF and PAZF were larger than 0 mV at the tested pH values, and they firstly increased and then decreased sharply with the increasing of pH, in which HOAZF and PAZF reached the highest Zeta potentials at pH 4 or so. The Zeta potential of HOAZF was smaller than that of PAZF over the tested pH range, apart from pH >11. The Zeta potential of HOAZF and PAZF tended to be the value equivalent to the isoelectric point at pH 12, which suggested that the neutralization ability of HOAZF for pollutants negatively charged was weaker than that of PAZF at the tested pH range.

PR by HOAZF

Impact of dosage

The performance of HOAZF for turbidity removal and PR was compared to those of PAZF and PAC in treating the simulated wastewater containing DDVP with a dosage of 0.685–6.85 mmol/L. PAZF gave higher 40% turbidity removal than PAC (Figure 5(a)) at the dosage 0.685 mmol/L. However, PAC gave larger PR than PAZF (Figure 5(b)) at lower dosages.

Generally, turbidity removal by coagulation is performed by a kind of comprehensive action of charge neutralization/adsorption, bridging, and sweeping. PAZF (Fu *et al.* 2012) was a coagulant composited by three metal ions of aluminum, zinc and iron, much more complex in composition than PAC, so, PAZF will produce more complicated hydrolysis products in wastewater than PAC which was only polymerized by aluminum. The hydrolysis products of PAZF contained gels and solids structures formed by organic and inorganic ions, and polynuclear substances with high positive valence (Bao *et al.* 2014; Golbaz *et al.*

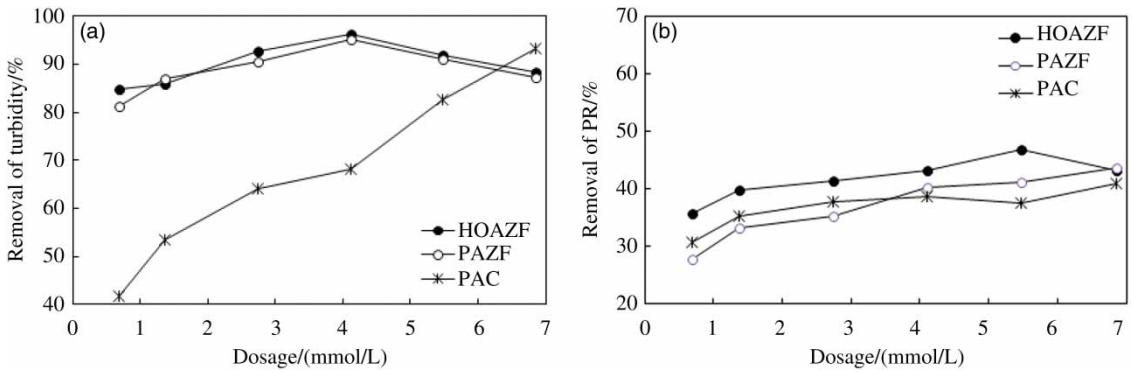

Figure 5 | Impact of dosage on removal of phosphorus and turbidity with HOAZF and PAZF in treating a simulated pesticide wastewater. TP = 664.8–676.3 mg/L.

2014; Zhang *et al.* 2015), thus giving better neutralization/adsorption for turbidity matters. Moreover, some zinc hydroxides and ferric hydroxides with amphoteric characteristics and some hydrolysis products of polynuclear or solids were formed during the hydrolysis of PAZF, so, turbidity removal by PAZF probably included charge neutralization/adsorption of fine particles and colloidal matters, and continuous adsorption/bridging for turbidity matters on flocs formed, etc. (Li 2012; Golbaz *et al.* 2014; Zhang *et al.* 2015). In addition, PAZF posed a kind of large uniform network structure consisting of some sort of cauliflower head with small size (Fu *et al.* 2012), thus giving excellent absorption for turbidity substances. Therefore, PAZF displayed much higher turbidity removal than PAC.

However, PR by coagulation was different from turbidity removal, in which the former included both coagulation and chemical processes. Generally, PR by a simple chemical process relates to a phase transfer of chemical precipitation in which some granular, insoluble phosphate will be formed in reactions between soluble phosphorus and inorganic salts (Hauduc *et al.* 2015). However, PR by coagulation is relatively complex, in which some discrete and colloid substances or some matters which are not easy to precipitate will become larger and larger flocs under action of coagulants (Keeley *et al.* 2016). Although the phase transfer was not the main process in coagulation, PR by coagulation was actually a simultaneous complex process involving non-phase transfer and phase transfer when many factors were changed, such as coagulation pH, phosphorus level, coagulant composition, etc. That is, PR by coagulation includes the following two behaviors: (1) coagulation function for solid colloidal phosphorus or particulate phosphorus (not easy to naturally precipitate) under the action of complex hydrolysis products of coagulants; (2) chemical precipitation for soluble phosphorus under the action of mononuclear inorganic salts produced by the hydrolysis process of coagulants.

Firstly, PAZF was compared with PAC. It can be considered that the tested wastewater in this work mainly contained organophosphorus (DDVP) and a little soluble inorganic phosphorus, apart from some other turbidity substances. DDVP exhibits lower solubility (about 10 g/L) in water at room temperature, but is easily hydrolyzed, especially at higher pH levels. So, the tested wastewater contained complex components, such as colloidal and soluble DDVP, the hydrolyzate of DDVP, and a small amount of inorganic phosphorus. The structural formula of DDVP used in this experiment is as seen in Formula (1):

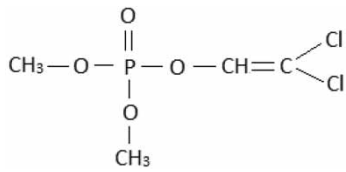

(1)

The electropositivity of P was enhanced by the electron-withdrawing substituent group (such as Cl) and oxygen atom on the double bond of P (Formula (1)). In addition, the electropositivity of P was probably increased by the complex hydrolysis process of DDVP. Therefore it can be considered that DDVP removal by coagulation rarely involved charge neutralization due to the charge repel action between DDVP and the hydrolysis products (often positively charged) (Golbaz *et al.* 2014; Zhang *et al.* 2015) formed by metal coagulant, such as HOAZF, PZAF and PAC. Moreover, the comparison of the results between Figure 5(a) and 5(b) also illustrates that the main DDVP removal mechanism by coagulation included adsorption/bridging and sweeping. So it can be seen that PR by PAZF was higher than that by PAC because the former formed much more complex hydrolyzate than the latter at higher dosages. Generally, mononuclear hydrolyzate formed by metal coagulants has chemical precipitation in removing phosphorus. The amount of mononuclear hydrolyzate formed by PAC (consisting of a single metal element) was perhaps more than that by PAZF at lower dosages, so chemical precipitation for PR by PAC was perhaps a little greater than that by PAZF, thus leading to a little higher PR by PAC than that by PAZF at lower dosages (Figure 5(b)). This was consistent with the results of Qiu (2000) who stated that PAC had higher removal of soluble inorganic phosphorus and total phosphorus.

Secondly, HOAZF was compared with PAZF. As also seen from the comparison between Figure 5(a) and 5(b), HOAZF gave 6% greater PR although it had almost the same turbidity removal as PAZF, thus indicating that some phosphorus was removed by chemical precipitation of HOAZF, not by coagulation together with turbidity

matters, which probably was due to the special function generated by the addition of PAM. This can be analyzed as follows. (1) As shown in Figures 1–4 and Table 1, HOAZF posed some special micro-characteristics, such as complex surface morphology (Figure 1), many small IR peaks and having no stretching vibration absorption peak of C = C double bond (Figure 2), having no characteristic diffractive peak of PAM (Figure 3), lower Zeta potentials (Table 1 and Figure 4), etc., which indicated that PAM was composited with metal elements during the composite reaction process, forming some complexes which were different from those in PAZF. (2) For HOAZF, the composite reaction between PAM and metal elements accelerated PR by chemical precipitation, which was probably due to the formation of much more mononuclear hydrolyzate promoted by the addition of PAM. (3) The addition of PAM reduced the positive charges carried by HOAZF (Table 1 and Figure 4). However, the results in Figures 1–3 also suggest that HOAZF gave much more complex composition than PAZF, so resulting in many more complex hydrolysis products formed by HOAZF than that by PAZF: HOAZF formed mononuclear hydrolyzate of metals, and also produced significantly more polynuclear hydrolyzate of metals, hydrolyzate of organic matters, and hydrolysis gels or solids of organic and inorganic matters during hydrolyzation. In addition, the molecular chain of the hydrolyzate formed by HOAZF was longer than that of PAZF due to the addition of PAM (Li 2012). Therefore, it can be inferred that HOAZF gave a better bridging performance than PAZF. Just as analyzed above that the main DDVP removal mechanism by coagulation included adsorption/bridging and sweeping, so HOAZF almost gave the similar turbidity removal to PAZF (Figure 5(a)), but having larger PR than PAZF.

At the same time, it can be seen that the desired dosage of HOAZF was far smaller than that of PAZF when reaching the same PR (Figure 5(b)) (1.37 vs 4.11 mmol/L if PR needed to reach 40%).

Impact of pH

Figure 6 shows the comparison of turbidity removal and PR between HOAZF, PAZF and PAC in treating a simulated wastewater containing DDVP with coagulation pH of 4–12.

As well known in the field of water coagulation, coagulation pH has a great impact on the composition and type of hydrolysis products of coagulants (Bao *et al.* 2014; Golbaz *et al.* 2014). Generally, for inorganic coagulants, increasing coagulation pH leads to both an increase of the amount of metal polynuclear hydrolyzate in the form of gels or solids and a gradual decrease of positive charges (Figure 4) carried by the hydrolyzate (Bao *et al.* 2014), thus resulting in both a decrease of charge neutralization function and an increase of the adsorption/bridging/sweeping action. Similarly, coagulation pH also has a great influence on PR by chemical precipitation. Generally, the efficiency of PR by chemical precipitation is higher at slightly lower pH range and neutral range, but weakened under strong alkaline conditions due to excess hydrolysis of coagulants.

As seen from Figure 6, coagulation pH almost displayed some impact on the elimination of turbidity and phosphorus by the three coagulants, but the impact on the latter was

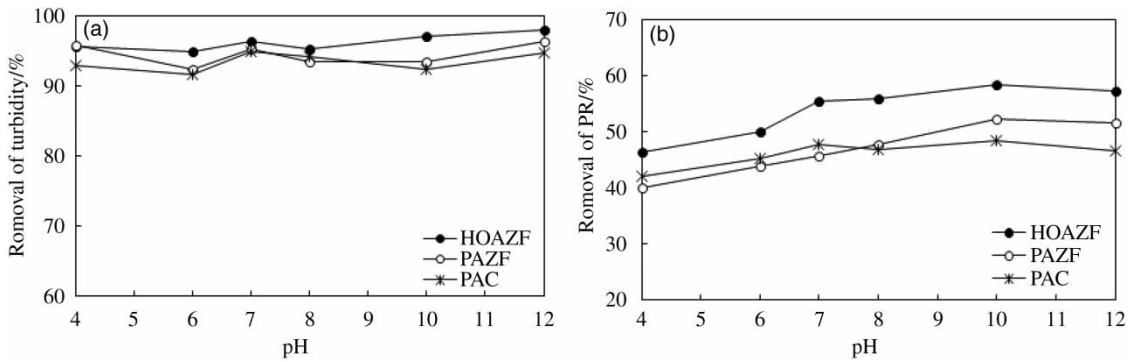

Figure 6 | Impact of coagulation pH on removal of phosphorus and turbidity by HOAZF and PAZF in treating a simulated pesticide wastewater. Dosage = 4.11 mmol/L.

larger than the former, which was consistent with the previous analysis: the removing mechanisms of turbidity were different from that of phosphorus, that is, turbidity was mainly removed by coagulation, while phosphorus was removed by a comprehensive process of coagulation and chemical precipitation, so, the impact of coagulation pH on PR was larger than that on the turbidity removal process.

Generally, the optimum coagulation pH often corresponds to the pH at which the solubility of the hydrolysis products was the smallest and less solid products were formed after adding coagulants to water samples. This optimum coagulation pH is often not within the strong alkaline range, which was somewhat different from the results in Figure 6(b): the three coagulants gave high PR in alkaline wastewater samples. This difference was consistent with the analysis mentioned above, further indicating that the insoluble organic phosphorus in the tested wastewater was mainly removed by adsorption/bridging/sweeping performed by polynuclear, gel-like or some solid hydrolysis products of coagulants during the coagulation process and a little soluble phosphorus was mainly removed by chemical precipitation acted by mononuclear hydrolyzate formed by coagulants. The reasons are as follows. DDVP hydrolyzed more rapidly in alkaline water samples and the positive charge carried by P in DDVP was also increased by the hydrolysis process in alkaline waters. Simultaneously, various gel-like products and a certain amount of solid products in the form of metal polynuclear polymers were formed during the hydrolysis process of inorganic coagulants. The amount of the gel-like and solid products was closely related to the pH of water samples, that is, the higher the pH, the more the formation of these products. So an adsorption/bridging/sweeping function was enhanced in alkaline water samples. Therefore, alkaline conditions are conducive to the removal of organic phosphorus which was positively charged and insoluble.

As also seen in Figure 6(b), coagulation pH has a different impact on PR by the three coagulants. (1) HOAZF almost had a similar suitable pH range to PAC (7–11), compared with 10–11 of PAZF. Under the main mechanism of adsorption/bridging/sweeping in removing organic phosphorus described above: like PAC, HOAZF probably formed a similar amount of mononuclear hydrolyzate of metals though much larger sized substances were formed in HOAZF, such as polynuclear hydrolyzate of three metals (Al, Fe and Zn), hydrolyzate of organic matters, and hydrolysis gels or solids of organic and inorganic matters, so, HOAZF gave higher PR by chemical precipitation which was related to the phase transfer process. It is clear that PR performed by chemical precipitation will be largely related to coagulation pH. Generally, PR by chemical precipitation will be increased under weakly acidic and neutral conditions, and be lowered by stronger alkaline conditions. So, HOAZF gave a similar optimal pH to PAC in PR. (2) PAZF gave a slightly lower PR than PAC at lower and neutral pH, and HOAZF gave higher PR than both PAZF and PAC over the whole pH range. PAC formed significantly more mononuclear hydrolyzate of Al during hydrolyzation under acidic and neutral conditions, thus resulting in excellent PR by PAC at lower and neutral pH. However, PAZF formed significantly more hydrolysis products (carrying many more positive charges) (Table 1 and Figure 4) which can exert better adsorption functions making it have no advantage in removing soluble phosphorus, so PAZF can exert a fully adsorption/bridging/sweeping performance only under alkaline conditions. While HOAZF had far more complex composition than PAZF and PAC, and gave a better comprehensive performance of coagulation and chemical precipitation in removing phosphorus, so HOAZF gave a higher removal of organic phosphorus than PAZF and PAC.

In order to further study the function of bridging and chemical precipitation of HOAZF in removing organic phosphorus, the impact of the phosphorus level on PR was analyzed as discussed in the following section.

Impact of phosphorus level

The performance of HOAZF for PR was compared to those of PAZF and PAC in treating a simulated wastewater containing DDVP with phosphorus level ranging from 41.1 to 664.8 mg/L (Figure 7).

HOAZF gave higher PR than PAZF and PAC at different phosphorus levels and dosages, in which PR by HOAZF reached 100% (Figure 7(b) when the dosage was up to a certain value (6.85 mmol/L) in treating a wastewater sample with lower phosphorus levels (40 mg/L). This demonstrated that HOAZF almost eliminated all

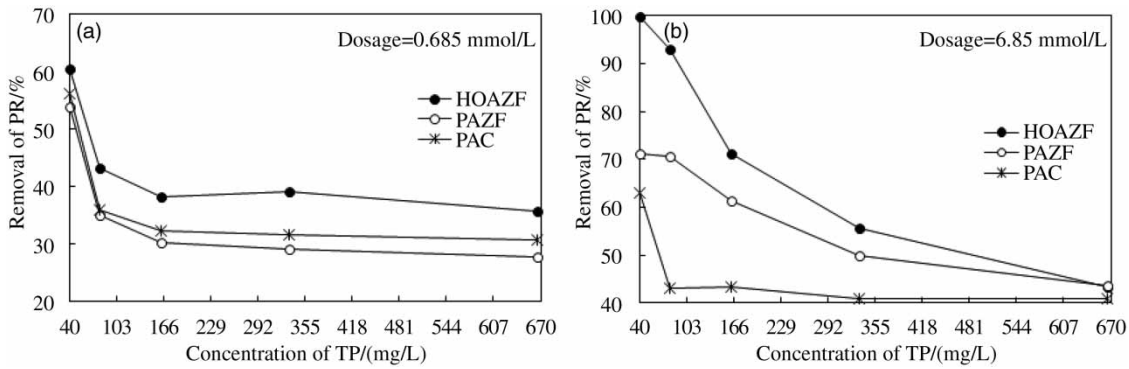

Figure 7 | Impact of phosphorus level on removal of phosphorus and turbidity with HOAZF and PAZF in treating a simulated pesticide.

kinds of phosphorus (involving insoluble and dissolved organic phosphorus, and inorganic phosphorus) by a comprehensive action including coagulation and chemical precipitation.

Figure 7 also shows that the dosage had a large influence on the relationship between PR and the phosphorus level. Just as previously described, the removal of organic phosphorus by coagulation was mainly dependent on adsorption/bridging and sweeping, together with a little chemical precipitation. The behavior of HOAZF for PR was only analyzed compared with that of PAZF, as follows. (1) The amount of soluble phosphorus was relatively greater when the phosphorus level was lower, therefore the PR probably mainly depended on both adsorption/bridging/sweeping and chemical precipitation: HOAZF only gave a little higher PR than PAZF due to the limited action of adsorption/bridging/sweeping and chemical precipitation of HOAZF at lower dosages (Figure 7(a)), while the excellent action of both adsorption/bridging/sweeping and chemical precipitation made HOAZF have much higher PR than PAZF at higher dosages (Figure 7(b)). (2) The action of adsorption/bridging/sweeping increasingly played a leading role due to the reduced amount of soluble phosphorus with the increasing phosphorus level; the action of adsorption/bridging/sweeping was mainly dependent upon the amount and characteristics of hydrolysis products of coagulants at lower dosages. So, the better performance of adsorption/bridging/sweeping developed by complex hydrolysis products made HOAZF always have higher PR than PAZF (Figure 7(a)). When the dosage was higher, the action of adsorption/bridging/sweeping mainly depended on the phosphorus level, so, PR by HOAZF gradually tended to be the same as that of PAZF (Figure 7(b)).

The suitable phosphorus level for HOAZF tending to reach a stable PR was slightly larger than that for PAZF which was larger than PAC (Figure 7(b)), thus suggesting that HOAZF gave a wider adaptation range of phosphorus level than PAZF at the same dosages. Similarly, PAZF gave a wider adaptation range of phosphorus level than PAC. In addition, compared to low dosages (Figure 7(a)), HOAZF gave an increasingly larger curve slope with the increasing of phosphorus concentration at higher dosages (Figure 7(b)), demonstrating that HOAZF can be adapted to a wider range of phosphorus levels with an increase of phosphorus concentration. This performance of HOAZF was probably due to its special characteristics in composition and complex hydrolysis process.

HOAZF had both higher removal of organic phosphorus and a wider range of suitable pH levels, and wider adaptable phosphorus levels, making HOAZF have more possibilities for treating complicated water qualities.

CONCLUSIONS

Complex composite reaction occurred between metals and PAM in HOAZF, forming some new crystalline substances and diffusive amorphous complexes, so leading to the following characteristics: complex surface morphology and relative lower Zeta potential, and promotion of PR by chemical precipitation due to the formation of much more

mononuclear hydrolyzate promoted by the addition of PAM.

PAZF posed far higher turbidity removal than PAC, with a difference of 40% at dosage 0.685 mmol/L, but they almost gave the similar PR at the same dosages. HOAZF almost displayed a similar turbidity removal to PAZF, but gave higher PR than PAZF over the whole dosage range, and the desired dosage of HOAZF was far smaller than that of PAZF when reaching the same PR. HOAZF and PAC almost posed the same suitable pH range of 7–11, compared with 10–11 of PAZF. HOAZF exhibited higher PR than PAZF and PAC at different phosphorus levels and dosages, in which PR by HOAZF reached 100% at a certain dosage (6.85 mmol/L). HOAZF posed a wider adaptation range of both pH and phosphorus level than PAZF, making HOAZF have many more possibilities for application in treating complex wastewater samples.

For the simulated wastewater mainly containing DDVP, the main PR mechanism by coagulation included adsorption/bridging and sweeping. PR by HOAZF coagulation was a simultaneous complex process involving non-phase transfer of adsorption/bridging/sweeping and phase transfer of chemical precipitation.

ACKNOWLEDGEMENTS

This research was supported by a Joint Project between University and Company (W14052 and W14097).

REFERENCES

Badawy, M. I., Montaser, Y. G. & Tarek, A. G. A. 2006 Advanced oxidation processes for the removal of organophosphorus pesticides from wastewater. *Desalination* **194**, 166–175.

Baldwin, C. J. 2012 *Sustainability in the Food Industry*, 2nd edn. Wiley-Blackwell, New Jersey, USA.

Bao, Y. P., Niu, J. F., Xu, Z. S., Gao, D., Shi, J. H. & Sun, X. M. 2014 Removal of perfluorooctane sulfonate (PFOS) and perfluorooctanoate (PFOA) from water by coagulation: mechanisms and influencing factors. *J. Colloid Interface Sci.* **434**, 59–64.

Cao, B. C., Gao, B. Y., Liu, X., Wang, M. M., Yang, Z. L. & Yue, Q. Y. 2012 The impact of pH on floc structure characteristic of polyferric chloride in a low DOC and high alkalinity surface water treatment. *Water Res.* **45**, 6181–6188.

Ding, S. M., Xu, D., Bai, X. L., Yao, S. C., Fan, C. X. & Zhang, C. S. 2013 Speciation of organic phosphorus in a sediment profile of Lake Taihu II. Molecular species and their depth attenuation. *J. Environ. Sci.* **25** (5), 925–932.

Du, X., Zhang, C. S., Wang, H. Y., Rong, H. W. & Zhang, Y. M. 2015 Phosphorus removal by biological-chemical strengthening process for municipal wastewater treatment. *Res. Environ. Sci.* **28** (9), 1474–1480.

EU Water Framework Directive 2000 Directive 2000/60/EC of the European Parliament and of the Council of 23 October 2000 establishing a framework for the Community action in the field of water policy. *Official Journal of the European Communities* **327**, 22.12.2000, pp. 38–51.

Fu, Y., Zhang, J. C., Wang, Y. Z. & Yu, Y. Z. 2012 Resource preparation of poly-Al–Zn–Fe (PAZF) coagulant from galvanized aluminum slag: characteristics, simultaneous removal efficiency and mechanism of nitrogen and organic matters. *Chem. Eng. J.* **203**, 301–308.

Fu, Y., Zhang, J. C., Wang, Y. Z., Yu, Y. Z. & Tan, J. 2014 Preparation and coagulation behavior of poly-Al-Zn-Fe coagulant from galvanized-aluminum-slag. *J. China Uni. Petrol.* **38** (1), 161–166.

Golbaz, S., Jafari, A. J., Rafiee, M. & Kalantary, R. R. 2014 Separate and simultaneous removal of phenol, chromium, and cyanide from aqueous solution by coagulation/precipitation: mechanisms and theory. *Chem. Eng. J.* **253**, 251–257.

Hauduc, H., Takács, I., Smith, S., Szabo, A., Murthy, S., Daigger, G. T. & Spérandio, M. 2015 A dynamic physicochemical model for chemical phosphorus removal. *Water Res.* **73**, 157–170.

Heiderscheidt, E., Saukkoriipi, J., Ronkanen, A. K. & Kløve, B. 2013 Optimisation of chemical purification conditions for direct application of solid metal salt coagulants: treatment of peatland-derived diffuse runoff. *J. Environ. Sci.* **26** (4), 659–669.

Huerta-Fontela, M., Galceran, M. T. & Ventura, F. 2008 Stimulatory drugs of abuse in surface waters and their removal in a conventional drinking water treatment plant. *Environ. Sci. Technol.* **42** (18), 6809–6816.

Keeley, J., Smith, A. D., Judd, S. J. & Jarvis, P. 2016 Acidified and ultrafiltered recovered coagulants from water treatment works sludge for removal of phosphorus from wastewater. *Water Res.* **88**, 380–388.

Kim, C. S., Rytuba, J. J. & Brown, G. E. J. 2004 EXAFS study of Hg(II) sorption to Fe- and Al-(hydr)oxide surfaces: I. effects of pH. *J. Colloid Interface Sci.* **271**, 1–15.

Li, X. X. 2012 *Studies on Turbidity Removal and Mechanisms by Enhanced Coagulation Using Composite Coagulants Containing Poly-dimethyldiallylammonium*. Doctor's Thesis, Nanjing University of Science & Technology, Nanjing, p. 40.

Li, B. & Brett, M. T. 2015 Characterization of the dissolved phosphorus uptake kinetics for the effluents from advanced nutrient removal processes. *Water Res.* **84**, 181–189.

Li, J., Yang, X. X. & Peng, Y. Z. 2002 *Microorganisms and Water Treatment Engineering*. Chemical Industry Press, Beijing, pp. 390–395.

Li, G. K., Hou, F., Guo, Z., Yao, G. Y. & Sang, N. 2011 Analyzing nutrient distribution in different particle-size municipal aged refuse. *Waste Manage.* **31**, 2203–2207.

Li, W., Wu, R. Q., Duan, J. M., Christopher, P. S. & van Leeuwen, J. V. 2016 Impact of prechlorination on organophosphorus pesticides during drinking water treatment: removal and transformation to toxic oxon byproducts. *Water Res.* **105**, 1–10.

Liu, Y., Wang, Y. L., Sheng, H., Dong, F. F., Zou, R., Zhao, L., Guo, H. C., Zhu, X. & He, B. 2014 Quantitative evaluation of lake eutrophication responses under alternative water diversion scenarios: a water quality modeling based statistical analysis approach. *Sci. Total Environ.* **468–469** (7), 219–227.

Lu, Y. Q. & Deng, Z. H. 1989 *Analysis of Practical Infrared Spectrum*. Publishing House of Electronics Industry, Beijing, pp. 24–84.

Meng, S. L., Qiu, L. P., Cheng, J. Z. & Xu, P. 2012 The research process of chemistry precipitation method in phosphorus removal in wastewater. *Chin. Agric. Sci. Bull.* **28** (35), 264–268.

Mudryk, Z. J., Perliński, P., Antonowicz, J. & Robak, D. 2015 Number of bacteria decomposing organic phosphorus compounds and phosphatase activity in the sand of two marine beaches differing in the level of anthropopressure. *Mar. Pollut. Bull.* **101**, 566–574.

Pan, J. R., Huang, C. & Lin, S. 2004 Re-use of fresh water sludge in cement making. *Water Sci. Technol.* **50** (9), 183–188.

Qiu, S. C. 2000 Chemical enhanced primary treatment (CETP) technology. *Chin. Water Wastewater* **16** (1), 26–29.

Remy, C., Miehe, U., Lesjean, B. & Bartholomaus, C. 2014 Comparing environmental impacts of tertiary wastewater treatment technologies for advanced phosphorus removal and disinfection with life cycle assessment. *Water Sci. Technol.* **69** (8), 1742–1750.

Saini, R. L. & Kumar, P. 2016 Simultaneous removal of methyl parathion and chlorpyrifos pesticides from model wastewater using coagulation/flocculation: central composite design. *J. Environ. Chem. Eng.* **4**, 673–680.

Schelske, C. L. 2009 Eutrophication: focus on phosphorus. *Science* **324** (5928), 722.

Schindler, D. W., Hecky, R. E., Findlay, D. L., Stainton, M. P., Parker, B. R., Paterson, M. J., Beaty, K. G., Lyng, M. & Kasian, S. E. M. 2008 Eutrophication of lakes cannot be controlled by reducing nitrogen input: results of a 37-year whole-ecosystem experiment. *Proc. Natl. Acad. Sci. USA* **105** (32), 11254–11258.

Strokal, M., Yang, H., Zhang, Y. C., Kroeze, C., Li, L., Luan, S. J., Wang, H. Z., Yang, S. S. & Zhang, Y. S. 2014 Increasing eutrophication in the coastal seas of China from 1970 to 2050. *Mar. Pollut. Bull.* **85**, 123–140.

Tan, X. P., Liang, S. Q., Cai, L. Y. & Zhang, G. W. 2011 Study of raman and IR spectra for Si-Al-Zr-O amorphous bulk in-situ crystallization. *Spectrosc. Spectral Anal.* **31** (1), 123–126.

Yan, W. L., Wang, Y. L. & Chen, Y. J. 2013 Effect of conditioning by PAM polymers with different charges on the structural and characteristic evolutions of water treatment residuals. *Water Res.* **47** (17), 6445–6456.

Ye, C. Y., Gu, J. C. & Zhang, J. 2009 Research phosphorus removal from life wastewater. *J. Xihua Uni.* **28** (6), 47–49.

Zhang, L. X., Bai, Y. F. & Han, X. G. 2004 Differential responses of N: P stoichiometry of Leymus chinensis and Carex korshinskyi to N additions in a steppe ecosystem in Nei Mongol. *Acta Bot. Sin.* **46** (3), 259–270.

Zhang, Y. L., Li, S. P., Wang, X. G. & Li, X. M. 2015 Coagulation performance and mechanism of polyaluminum ferric chloride (PAFC) coagulant synthesized using blast furnace dust. *Separ. Purif. Technol.* **154**, 345–350.

Zhao, H. C., Li, Q. & Wei, Z. Q. 2010 Synthesis and performance of polyacrylamide. *Chin. Synth. Resin Plastics* **6**, 25–29.

Zhou, Q., Han, S. Q. & Yan, S. H. 2015 Simultaneous removal of phosphorus and algae in eutrophic waters by modified complexes of aluminium polychlorid and clay. *Environ. Chem.* **34** (11), 2059–2066.

Zielinski, P. & Jekatierynczuk-Rudczyk, E. 2015 Comparison of mineral and organic phosphorus forms in regulated and restored section of a small lowland river (NE Poland). *Ecohydrol. Hydrobiol.* **15**, 125–135.

First received 15 June 2016; accepted in revised form 13 December 2016. Available online 8 February 2017